Journal of Medicinal and Chemical Sciences 6 (2023) 1714-1726

Journal of Medicinal and Chemical Sciences

Journal homepage: http://www.jmchemsci.com/

Original Article

Synthesis, Characterisation, and Biological and Computational Studies of Novel Schiff Bases from Heterocyclic Molecules

Seta Azad Aghaward[1], Layla Jasim Abbas[1,*], Kawkab Ali Hussein[2]

[1]*Pharmaceutical Chemistry Branch, Pharmacy College, The University of Basrah, Basrah, Iraq*
[2]*Department of Chemistry, College of Education for Pure Sciences, The University of Basrah, Basrah, Iraq*

ARTICLE INFO

Article history

Receive: 2022-10-13
Received in revised: 2022-11-21
Accepted: 2022-12-24
Manuscript ID: JMCS-2211-1903
Checked for Plagiarism: **Yes**
Language Editor:
Dr. Fatimah Ramezani
Editor who approved publication:
Dr. Ali Hammood

DOI:10.26655/JMCHEMSCI.2023.8.1

KEYWORDS

Green Synthesis
Triazole Schiff Base
Anticancer
Molecular Docking

ABSTRACT

Four new Triazole Schiff Bases were synthesized through the green condensation and were structurally confirmed by mass spectroscopy, IR, ^{1}H NMR, TGA, and DSC. The chief advantages of the reported technique were its working ease, very mild reaction conditions, short reaction time, and high yield. Quantum chemical calculations were applied to investigate the optimized geometry and electronic structure of the compounds, **S1-S4**. DFT/B3LYP/6-31+G (d), was performed to determine the chemical quantum descriptors (CQDs). An analysis of the CQDs showed that the **S1** compound had a higher molecular stability. The findings of the computational research revealed that there was a close interaction between the theoretical and experimental data. The synthesized compounds were studied for their anticancer activity against two cell lines, MCF-7 and HepG2. The results revealed that the **S3** and **S4** compounds had a remarkable activity, with IC_{50} of 64.64 µg/mL and 23.52 µg/mL, respectively, thus, making them crucial components for anticancer medicines in future studies. Molecular docking tests were carried out on the **S3** and **S4** compounds with the receptors 5EKN and 3PP0. The results exposed that the compounds were effective in inhibiting the receptors with a good binding energy to confirm their anticancer activity.

GRAPHICAL ABSTRACT

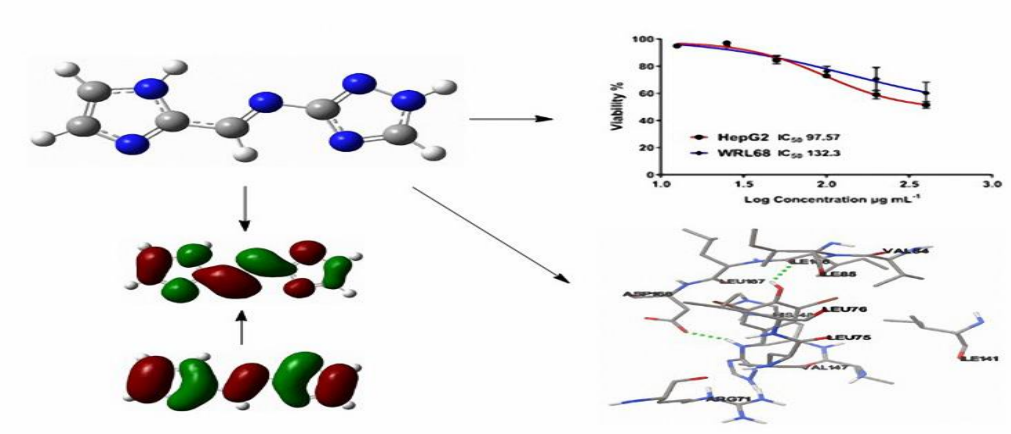

* Corresponding author: Layla Jasim Abbas
✉ E-mail: Email: layla.abbas@uobasrah.edu.iq

Introduction

The products obtained from the condensation of carbonyl and the primary amine compounds are called Schiff bases, named after Hugo Schiff, who recorded the first synthesis of Schiff bases (imines) in 1864 [1]. A Schiff base is considered as an aldehyde that bears an azomethine -N=CH- group, which plays a key role. Schiff bases are well known for their wide-spectrum potential as chemotherapeutic agents [2, 3]. Heterocyclic Schiff bases, such as triazole Schiff base derivatives are widely known for their potential as antibacterial, anti-inflammatory, anticoagulant, and anticancer drugs and antiviral agents [4, 5]. In recent years, studies on triazole Schiff base derivatives have been gaining increasing attention. Therefore, the preparation and characterisation of triazole Schiff base derivatives are of great significance due to their ability to help in the synthesis of several bioorganic conjugates with different moieties, in addition to their greater tendency to form hydrogen bonds, thereby improving their pharmacokinetic, pharmacological, and toxicological properties in addition to their physicochemical properties [6-9]. Consequently, 1,2,4- triazole derivatives are included in several drugs like fluconazole, voriconazole, and itraconazole that are used in the treatment of many diseases. However, experimental, quantum chemical, and molecular docking methods have been combined to create a triple hybrid strategy to examine these compounds. Computational studies, such as the density-functional theory (DFT), have been used to study the structure-property relationship, alongside with molecular docking to highlight the potential to confirm a good interaction between receptors and compounds [10-12]. In this study, triazole Schiff base derivatives were initially synthesised and characterised. They were then evaluated for their anti-cancer activity on the MCF-7 and HepG2 cell lines using an MTT assay and compared to the HdFn and WRL68 normal cell lines. In addition, their HOMO–LUMO energy gap, chemical hardness and global softness were investigated using the density-functional theory (DFT) to determine the stability of the compounds. A molecular docking study was performed to investigate their interaction and binding activity with target receptors.

Materials and Methods

1,2,4-Triazole-3-amine, imidazole-2-carbaldehyde, 5-bromofuran-2-carbaldehyde, 3,5-dibromo-4-hydroxybenzaldehyde, and terephthalaldehyde, with 96-98% purity, were used without further purification (their melting points were examined and were found to be: 157-159 °C, 206-209 °C, 82-85 °C, 181-185 °C, and 113-117 °C, respectively). Nuclear magnetic resonance (NMR) spectroscopy was performed at the Department of Chemistry, College of Education for Pure Sciences, University of Basrah: The ^{1}H-NMR spectra were recorded using a Bruker Avance NEO 400 (400 MHz) spectrometer. In assigning the ^{1}H-NMR spectra, the chemical shift information (δH) for each resonance signal was given in units of parts per million (ppm) relative to trimethylsilane (TMS), where (δH) = 0.00 ppm. The number of protons (n) for a reported resonance signal was indicated as nH from their integral value, and the multiplicity was symbolised by the following abbreviations: s = singlet and d = doublet. A thermal gravimetric analysis (TGA-DSC) was performed at the Chemistry Department, College of Pure Sciences, Basrah University, using the TGA-50 thermal analysis system and DSC-60 Plus/60 A Plus differential scanning calorimeter from Japan. The infrared (IR) spectra measurements were run using a Bruker/FT-IR Affinity-1 spectrophotometer at the College of Pure Sciences, Thi Qar University. The mass spectra were recorded using a Shimadzu model GCMS-QP2010 plus at Samarah University. Biological activities were carried out at Tehran University, Iran.

Synthesis of compounds

Four compounds were prepared by the condensation of the amine (**I**) with the aldehyde (**II-V**), (Scheme 1) in a green way (no catalyst or reagent, small quantity of solvent and short reaction time, easy purification process, and high yield).

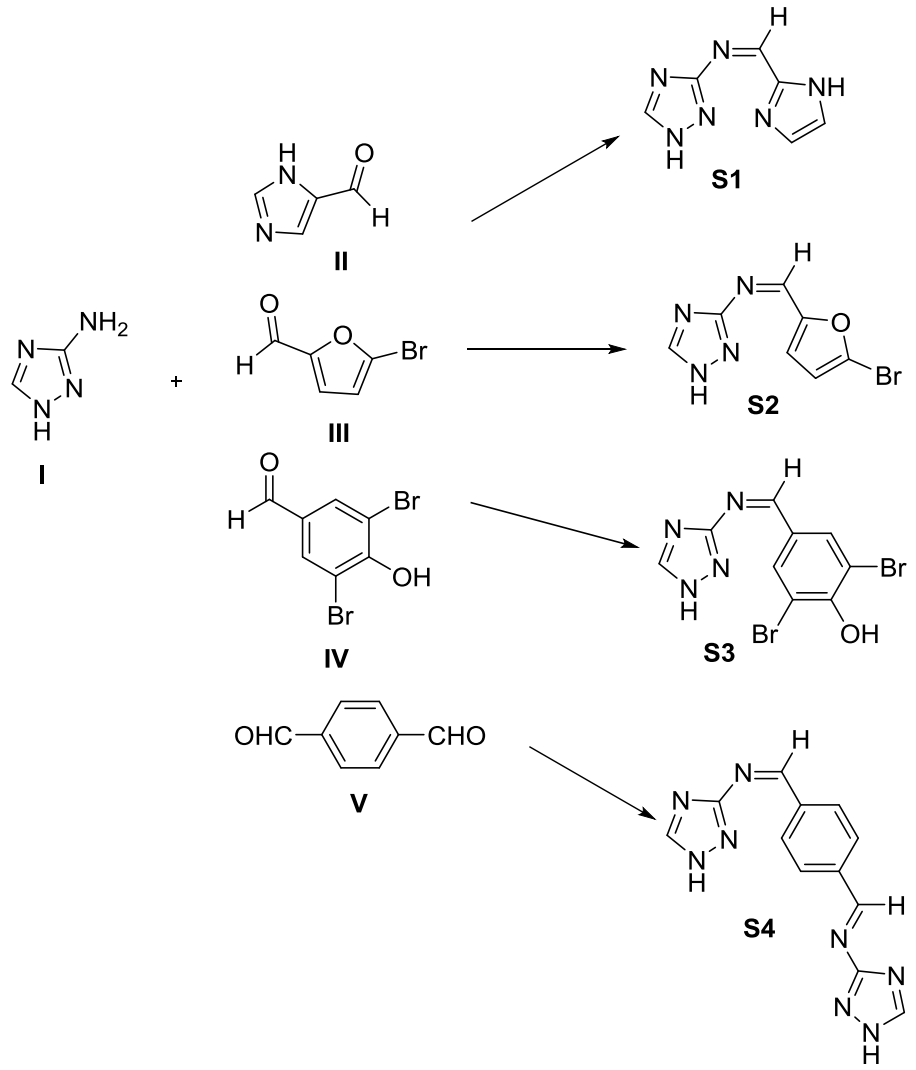

Scheme 1: Chemical structure of the synthesised triazole Schiff bases (**S1**-**S4**)

*(Z)-N-((1H-imidazol-2-yl)methylene)-1H-1,2,4-triazol-3-amine (**S1**)*

3-Amino-1*H*-1,2,4-triazol (0.192 g, 2.286 mmol) and 2-imidazolecarboxaldehyde (0.220 g, 2.286 mmol.) were mixed in a round-bottom flask. Then, 15 mL of absolute methanol was added to the mixture. The reaction mixture was refluxed for 3 hours, followed by TLC (performed using Merck 60 F_{254} nm silica-coated aluminium sheets, 1:1 ethyl acetate in dichloromethane). The mixture was left for a day to complete the precipitation. Thereafter, the precipitate was washed with cold methanol to get rid of the residual aldehyde and amine. The light brown product weighed 0.25 g (1.541 mmol, 67 %, mp. >205 ºC). The compound was slightly soluble in methanol, soluble in DMSO, and not soluble in chloroform. The desired pure product was characterized by ^{1}H-NMR spectra (Figure S1, Supporting information).

*(Z)-N-((5-bromofuran-2-yl)methylene)-1H-1,2,4-triazol-3-amine (**S2**)*

3-Amino-1*H*-1,2,4-triazol (0.192 g, 2.286 mmol) and 5-bromo-2-furaldehyde (0.40 g, 2.286 mmol) were mixed in a round-bottom flask. Then, 15 mL of absolute methanol was added. The reaction mixture was refluxed for 3 hours, followed by TLC (performed using Merck 60 F_{254} nm silica-coated aluminium sheets, 1:1 ethyl acetate in dichloromethane). The mixture was left for a day to complete the precipitation. Next, the precipitate was purified using column chromatography (SiO_2, 0-70% absolute methanol in dichloromethane). The brown yellowish product weighed 0.414 g (1.717 mmol, 75 %, mp.

165-169 °C). The compound was soluble in methanol, but not in chloroform. The desired pure product was characterized by ^{1}H-NMR spectra (Figure S2, Supporting information).

*(Z)-4-(((1H-1,2,4-triazol-3-yl)imino)methyl)-2,6-dibromophenol (**S3**)*

3-Amino-1*H*-1,2,4-triazol (0.192 g, 2.286 mmol) and 3,5-dibromo-4-hydroxybenzaldehyde (0.640 g, 2.286 mmol) were mixed in a round bottom flask. Then, 15 mL of absolute methanol was added. The reaction mixture was refluxed for 3 hours, followed by TLC (performed using Merck 60 F_{254} nm silica-coated aluminium sheets, 1:1 ethyl acetate in dichloromethane). The mixture was left for a day to complete the precipitation. After that, the precipitate was purified using column chromatography (SiO_2, 0-70% absolute methanol in dichloromethane). The light-yellow product weighed 0.68 g (1.965 mmol, 86 %, mp. 160-167 °C). The compound was soluble in methanol, but not in chloroform. The desired pure product was characterized by ^{1}H-NMR spectra (Figure S3, Supporting information).

*N,N'-(1,4-phenylenebis(methanylylidene))bis(1H-1,2,4-triazol-3-amine) (**S4**)*

3-Amino-1*H*-1,2,4-triazol (0.630 g, 7.493 mmol) and terpthaldehyde (0.50 g, 3.728 mmol) were mixed in a round-bottom flask. Then, 20 mL of absolute methanol was added. The reaction mixture was refluxed for 3 hours, followed by TLC (performed using Merck 60 F_{254} nm silica-coated aluminium sheets, 1:1 ethyl acetate in dichloromethane). The mixture was left for a day to complete the precipitation. Then, the precipitate was washed 3 times (3×10 mL) with cold methanol to get rid of the residual aldehyde and amine. The light-yellow product weighed 0.65 gm (2.441 mmol, 65 %, mp. > 205 °C), was soluble only in DMSO, but was not soluble in methanol, ethanol and chloroform or dichloromethane. The desired pure product was characterized by ^{1}H-NMR spectra (Figure S4, Supporting information).

Results and Discussion

The main change occurred in the NMR chart and which helped to explain the reaction taken place was the disappearance of the aldehyde band, which generally appeared around 10 ppm in the ^{1}H-NMR, and the appearance of the imine (HC=N) signal [13] at around 9 ppm.

The bending vibration of N–H in the primary amines was observed in the region of 1650-1580 cm $^{-1}$. Most of the secondary amines do not show a band in this region, and tertiary amines never show a band in this region (This band is possibly very sharp and close enough to the carbonyl region to cause researchers to interpret it as a carbonyl band). The aromatic Schiff-bases were investigated using the IR technique, and a band of medium intensity was indicated in the double-bond stretching region at 1613-1631 cm^{-1} for the C=N [14, 15]. The characteristic FT-IR assignments of the compounds (**S1**-**S4**) in Figures S5, S6, S7 and S8 (Supporting information), depicted a strong band at 3460 cm^{-1} assigned to (NH). The imine (C=N) band of the Schiff base moiety appeared as a strong band at (1630 and 1598) cm $^{-1}$ [16]. Aromatic aldehydes usually show a sharp band at 1720–1680 cm^{-1} due to carbonyl group stretching [15]. The carbonyl band (C=O) of the aldehydes used in this study showed sharp signals at 1660 cm^{-1} (2-imidazolcarboxyaldehyde), 1660 cm^{-1} (5-bromo-2-furaldehyde), and 1670 cm^{-1} (3,5-dibromo-4-hydroxybenzaldehyde). This band shifted to a lower wavenumber (lower frequency and energy) at 1621 cm^{-1} (**S1**), 1608 cm $^{-1}$ (**S2**), 1613 cm $^{-1}$ (**S3**), and 1609 cm $^{-1}$ (**S4**).

The mass spectra in Figures S9, S10, S11, and S12 (Supporting information), for the compounds S1-S4, respectively, demonstrated the existence of the required masses expected for the desired compounds. The thermal analysis results of the synthesised Schiff bases (**S1**-**S4**) are presented in Figures S13, S14, S15, S16, S17, S18, S19, and S20 (Supporting information). Compound **S1** was the condensation product of an amino triazole with the aldehyde, diazole carbaldehyde.

The DSC spectrum indicated the formation of a Schiff base with a melting point ranging from 225 °C to 325 °C. The TGA showed two stages of decomposition, one at the temperature range of

148.6 -333.6, DTG 250 °C (50% weight loss of the first stage), gradually losing the imidazole segment from the Schiff base. Besides, compound **S2** was the condensation product of 3-amino1,2,4 triazole with 5-bromo-2-furfuraldehyde. The DSC thermogram showed two exothermic peaks, one at 174-190 °C, which could be related to the loss of HCN from the formed Schiff base, and the second at 231-266 °C, which could be related to the loss of the triazole segment. These were in good agreement with the TGA analysis results. The TGA thermogram showed two main decomposition loss peaks, one at 225.52-331.78 °C. This could be related to the calculated loss of HCN:11.2% found from TGA: 14.1%. The second loss peak at 386.76-597.02 could be related to the loss of the triazole segment (calculated: 29% found from TGA: 26.48%). The residue was about 60% related to the bi(bromofuraldehyde) (60.9%). Likewise, compound **S3** was product of the condensation of 3-amino 1,2,4-triazole with 3,5-dibromo-4-hydroxy benzaldehyde. The DSC showed a main melting /decomposition peak at 229.8-279.3 °C.

The TGA analysis showed three decomposition loss peaks, the first at 180-272 °C related to the loss of the triazole Schiff base segment, followed by the second one at 272 °C, which could be related to the loss of 2,6-dibromophenol (calculated as 72 % found from TGA: 70%). In addition, compound **S4** was the condensation product of 3-amino1,2,4 triazole with terphthaldehyde. The DSC showed a melting/decomposition exothermic peak at 360.7-383.9 °C. The TGA showed a sharp loss peak at 200-374.91, which could be related to the loss of two molecules of HCN (calculated as 20.3% found from TGA: 19%).

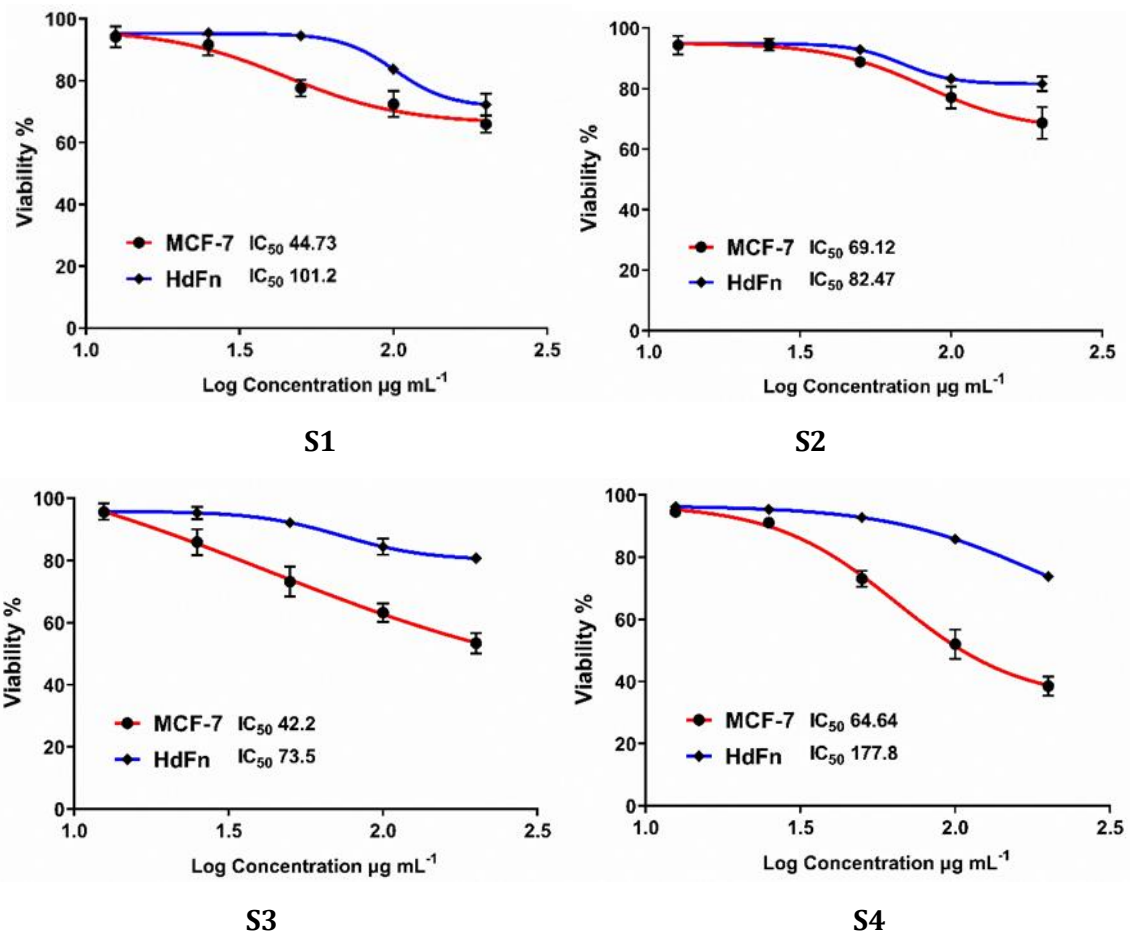

Figure 1: Cytotoxicity of compounds and with MCF-7 and HdFn normal cell

Biological activity

The *in vitro* anticancer activity of the synthesized compounds at different concentrations was tested on MCF-7 and HepG2 cells with 24 hours of incubation. All the compounds resulted in a decrease in cell viability in a dose-dependent manner as follows: **S4**> **S3**> **S2**> **S1**, and the **S4** compound resulted in a significant decrease in the survival rate of the MCF-7 cells in a dose-dependent manner with IC_{50} at 64.64 µg /mL, with minimal and moderate cytotoxicity exhibited on normal cell lines. It had a more cytotoxic effect on HdFn, as depicted in Figure 1, compared to the other compounds, as listed in Table 1. In contrast, in Figure 2, both the **S4** and **S3** compounds induced significant cytotoxicity on the HepG2 cell line, while the normal cell line of WRL-68 hepatic cells exhibited only the moderate susceptibility. The corresponding IC_{50} values are summarised in Table 2. The result showed that the **S4** compound significantly inhibited the proliferation of HepG2 cells, while its cytotoxicity on the normal cell line of WRL-68 hepatic cells compared to IC_{50} 23.52 µg /mL value of the compounds toward HepG2 cells was shown to be weak and moderate. Based on the results obtained from the MTT assay, the prepared compounds showed a dose-dependent cytotoxic activity against cancer cells. These results indicate that these compounds have the potential to be anti-cancer agents in view of their potent cytotoxicity and antitumor activity in the order of **S3**> **S1**> **S4**> **S2** [17-19].

Table 1: Cytotoxic effects of compounds against MCF-7 and HdFn normal cells

Compound	MCF-7	HdFn
	IC_{50}	
S1	44.73	101.2
S2	69.12	82.47
S3	42.20	73.50
S4	64.64	177.8

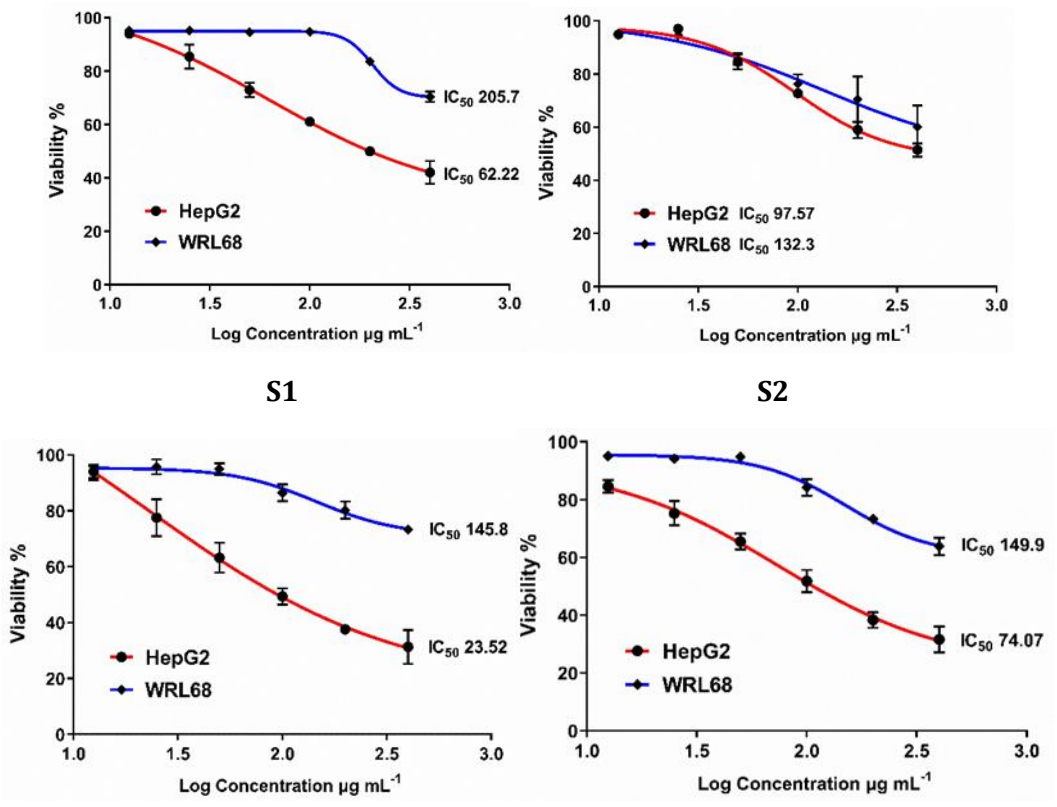

Figure 2: Cytotoxicity of compounds with HepG2 and WRL68 normal cell

Table 2: Cytotoxic effects of compounds against HepG2 and WRL68 normal cell

Compound	HepG2	WRL68
	IC_{50}	
S1	62.22	205.7
S2	97.57	132.3
S3	23.52	145.8
S4	74.07	149.9

Statistical analysis

The averages and standard deviations (SD) for three separate studies were used to represent the experimental values. The GraphPad Prism 7 was used to carry out the analysis of variance (ANOVA), where $p < 0.0001$ was considered as statistically significant.

Molecular docking studies

In the current study, the **S3** and **S4** compounds were shown to have the best cytotoxic effects on MCF-7 and HepG2 *in vitro*, as observed from their respective experimental anticancer activity. The **S3** and **S4** compounds were chosen as inhibiting receptors of gene expressions in MCF-7 [20] and HepG2 [21]. To investigate the ability of these compounds to bind to and inhibit 5EKN and 3PP0, a similar molecular docking study was performed. This study was aimed at evaluating the potential binding affinities, modes, and interactions of the new compounds against those of special proteins. Docking simulations were carried out using the Auto Dock 4.2 software [22] to characterise the interactions between the most potent **S4** and **S3** compounds and the active sites of the receptors following the docking protocol to achieve the docking study of **S3** and **S4** into the active site of proteins. The crystallographic structures of the protein kinase, 5EKN, and the human epidermal growth factor receptor, 3PP0, were chosen as the templates to model the study of the compounds. The cell cycle, apoptosis, and growth factor-mediated cell survival, which are hallmarks of hepatocellular carcinoma HepG2 and breast cancer MCF-7, were all regulated by these receptors. Hindrance of this protein by employing an impeding receptors pathway has attracted wide interest as a way to deal with hostility to disease treatment. Furthermore, a restriction on receptor signalling can alter or stop development. The receptors were recovered from the protein information bank [23]. After 10 runs, the ligand-receptor complexes were further analysed using Auto Dock 4.2. The molecular docking analysis helped to identify different types of binding interactions, such as H-bonding, hydrophobic, and electrostatic interactions. To select the greatest docking pose with the lowest energy, the docking process was repeated numerous times. The molecular docking of **S3** showed a moderate fit into the binding of the active 5EKN receptor site with an energy affinity of -6.87 KJ/mol, where the amino acid residue and **S3** showed two interactions (H-bonding) with the amino acids, Asp188 and ILE. Meanwhile, the affinity energy of the 3PP0 receptor with **S4** exhibited good binding at 7.3KJ/mol. They formed two hydrogen bonds with ARG849 and ASP845. Overall, the outcomes demonstrated that the **S3** and **S4** compounds tested with the receptors had good docking scores. The stability of the ligand-protein complex was increased as a result which hindered the receptor signalling pathways associated with cancer. The findings demonstrated that these compounds may play a role in the apoptotic cell death process in cancer. All the data are presented in Table 3 and Figure 3.

Computational details

Calculations were done using DFT to determine the minimum geometrical structure at cam-b3lyp/6-31g (d) level of theory by Gaussian 09 programs [24]. Theoretical parameters were used to help describe the molecular structure of the investigated compounds. To study the properties of the synthesised compound, the highest molecular occupied orbital (HOMO), the lowest molecular unoccupied orbital (LUMO), and some chemical quantum descriptors (CQDs)

were theoretically estimated. Table 3 and Figure 4 show the computed properties using the same technique as the geometry optimization.

In addition, the estimated information helped in further describing the molecular characteristics of the compounds. The values of the electronic properties of the compounds are displayed in Table 4 and Figure 5 HOMO and LUMO energies: The ability of a molecule to interact with other molecules is generally represented by the values of the highest and the lowest occupied molecular orbital energies (E_{HOMO} and E_{LUMO}), respectively. The electron-donating capability of a molecule is represented by the term E_{HOMO}. A molecule with a high E_{HOMO} value has a strong ability to donate electrons to a lower energy molecule (an empty orbital). The ability of a molecule to receive electrons from an energetic molecule is greatest when it has a low E_{LUMO} value (an occupied orbital) [25, 26]. The **S4** compound appeared to have a low E_{LUMO} value compared with the other compounds. However, the **S3** compound had the highest E_{HOMO}. Energy gap (ΔE): The HOMO-LUMO energy separation has been a basic indicator of kinetic stability. A chemically-reactive molecule has a low HOMO-LUMO gap [27]. In addition, the ΔE is primarily capable of measuring electrical conductivity; an increase in conductivity is correlated with a decrease in the band gap. It is possible to understand the relationship between conductivity and ΔE using Equation 1.

$$\sigma \infty \exp (\Delta E / kT) \quad (1)$$

Table 3: The selected parameters of the compounds with best conformer with proteins

Compound	Pdb	B.E	Ki uM	I.E	V+B+D	E.E	F.T.I	No. of H-B
S3	5EKN	-6.87	9.28	-8.01	-7.40	-0.64	-0.11	2
S4	3PP0	-7.30	4.45	-8.51	-7.06	-0.64	-0.28	2

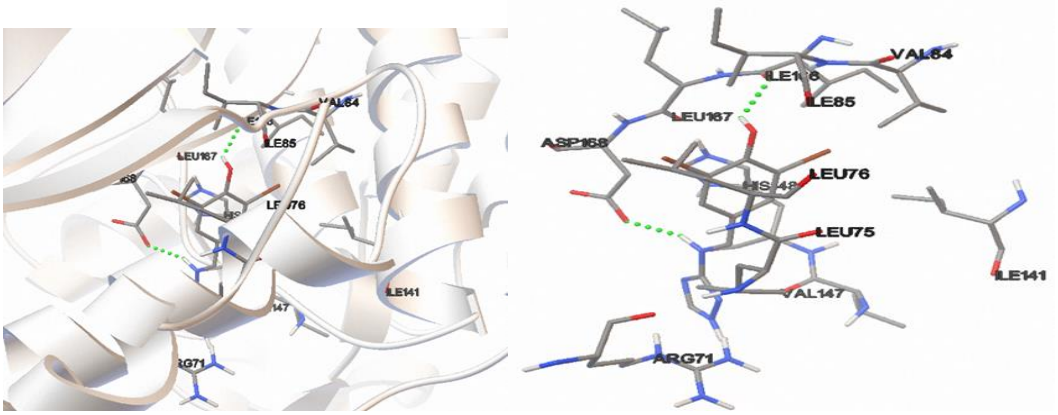

A. Stick representation B. Ribbon format

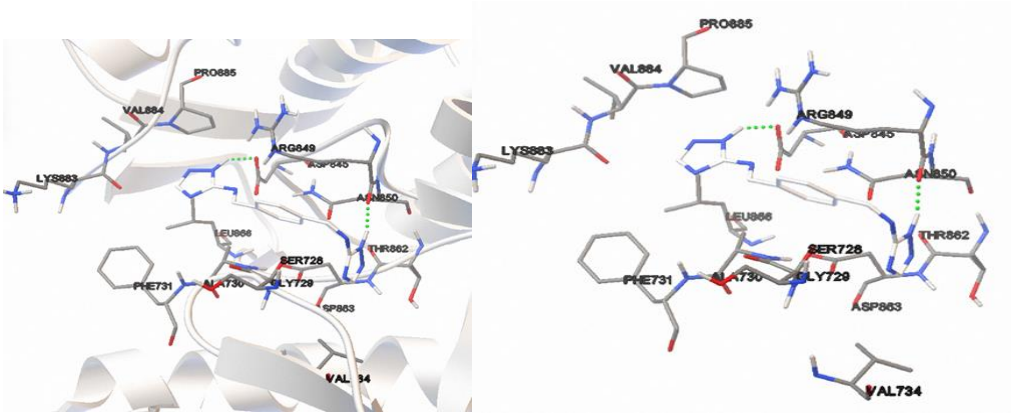

A. Stick representation B. Ribbon format

Figure 3: Position and orientation for compounds **S3** and **S4** with protein residues

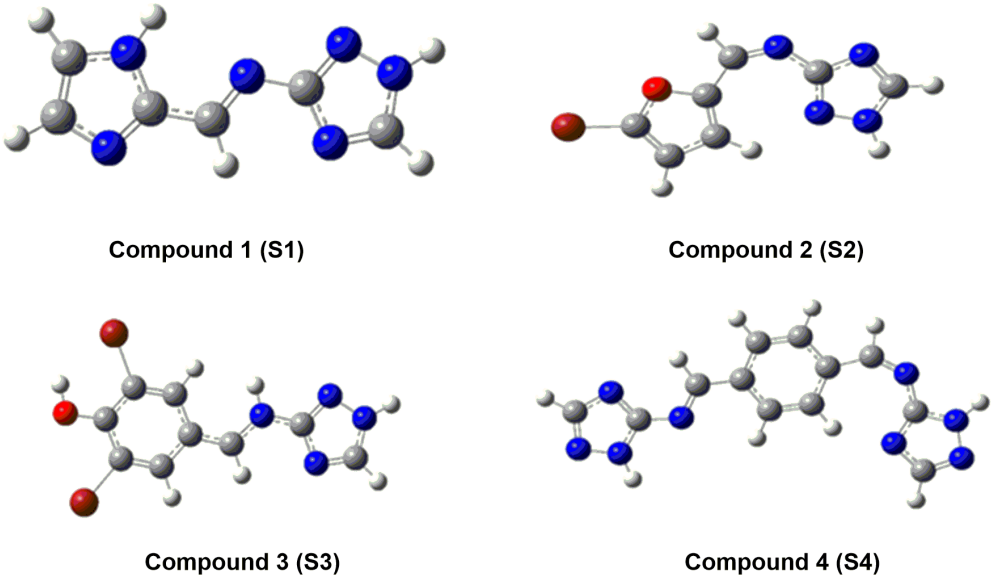

Figure 4. The modeling structures of the triazole-based Schiff base (**S1-S4**)

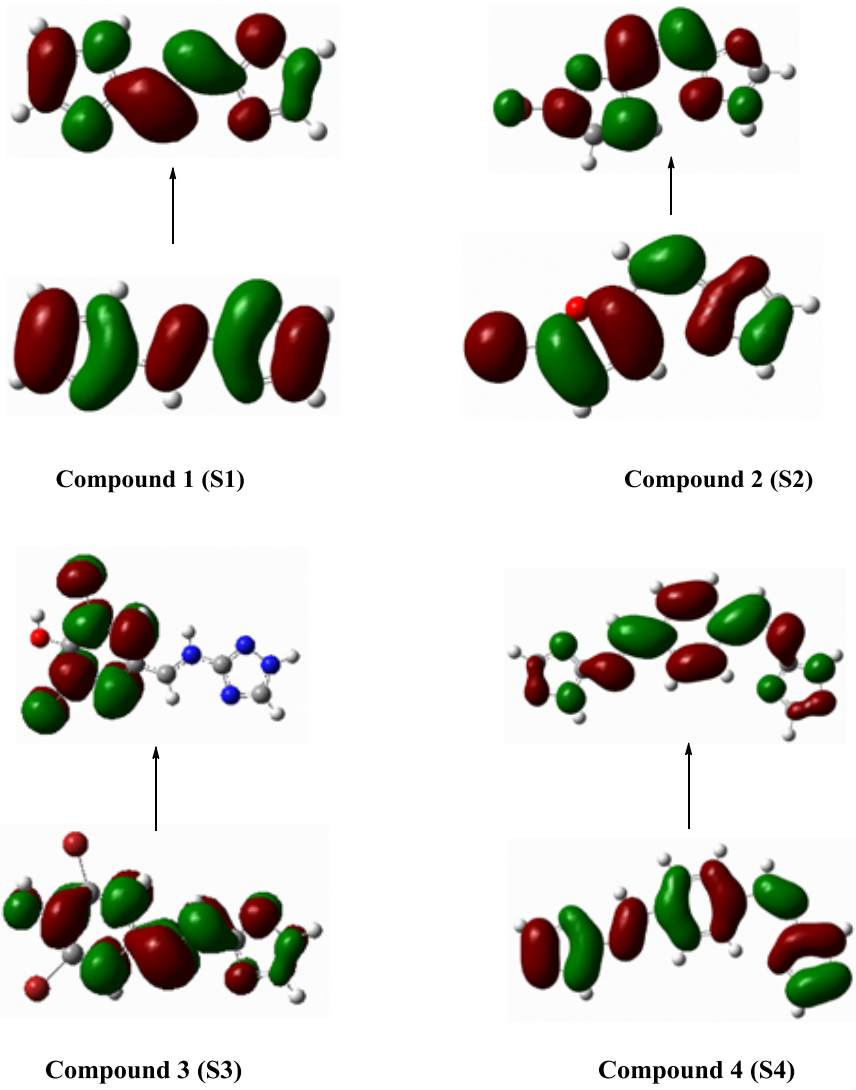

Figure 5. The HOMO-LUMO of the triazole-based Schiff bases (**S1-S4**)

Where, σ is the electrical conductivity, and k is the Boltzmann constant. This confirms a reduction in band gap, ΔE, which suggests a rise in the electrical conductivity [28]. According to the above data, **S3** had more chemical activity and electrical conductivity than the other studied compounds. Furthermore, the HOMO and LUMO energy values were used to calculate the global chemical reactivity parameters, such as electrochemical potential (μ), chemical hardness (η), and electrophilicity (ω). The electrochemical potential can be represented by $\mu = (E_{HOMO}+E_{LUMO})/2$, which indicates the propensity to release electrons [29]. In this set, the S4 molecule had a high electrochemical potential absolute value, and would behave as a strong electron-acceptor molecule, whereas the **S3** molecule had a low value for μ, and therefore, would behave as a strong electron-donor molecule. The chemical hardness can be defined as the capacity of a molecule to resist changing electron density with its surroundings. It is expressed as $\eta = (E_{LUMO} - E_{HOMO})/2$ [30]. It has to do with how chemical systems behave in terms of stability and reactivity. A hard molecule has a HOMO-LUMO gap that is greater than one. A molecule becomes more stable the larger its gap and it requires more energy to be excited [31]. As seen in Table 4, **S1** had a high chemical hardness compared with the other molecules. Therefore, **S1** was a hard and more stable molecule than the others. Electrophilicity (ω) measures the energy stability of a molecule when it gains extra electron density. It is expressed as $\omega = \mu^2/2\eta$. The electrophilicity of the compounds in decreasing order was as follows: **S4**, **S2**, **S1**, and **S3**. As a result, **S3** was generally less reactive and more stable when accepting electrons. The contribution in polar Diels-Alder reactions is simple for strong electrophiles like **S4** (ω = 3.4872 eV), for example. **S3**, ω = 0.8300 eV, is a weakly electrophilic material that cannot act in polar reactions [30].

Table 4: Ground state properties of the triazole-based Schiff base using B3LYP/6-31+g (d,p)

Compound	HOMO eV	LUMO eV	ΔE eV	ω	η	μ
S1	-7.2790	-0.2258	7.0532	1.9963	3.5266	-3.7524
S2	-7.7361	-0.8707	6.8654	2.6974	3.4327	-4.3034
S3	-5.2436	0.7738	6.0174	0.8300	3.0087	-2.2349
S4	-7.7225	-1.5537	6.1688	3.4872	3.0844	-4.6381

Conclusion

In this study, four compounds were synthesised, characterised, and tested for their anti-tumour activity against the MCF-7 and HepG2 cell lines. As a result of the anticancer screening of the four compounds, the evaluated compounds showed specific anticancer effects, especially the **S3** and **S4** compounds, with IC_{50} 64.64 μg/mL and IC_{50} 23.52 μg/mL, respectively. In contrast, the compounds were non-cytotoxic activates to normal human cells, namely, HdFn and WRL-68 cells. The molecular docking between the **S3** and **S4** compounds with the receptors of 5EKN and 3PP0 was examined to approve the experimental anticancer activity results. The study revealed that the **S3** and **S4** compounds accommodated the receptor sites, formed H-bonds, and showed better interaction with good binding energy. In general, the study offers good experimental data and theoretical information for future advancement and application as anticancer medications. To understand the nature and reactivity of the molecule, the chemical quantum descriptors (HOMO, LUMO, ΔE, ω, η, and μ) were theoretically calculated to examine the characteristics of the compounds. The greater the ΔE, the more stable will be the compound. The ΔE is primarily capable of measuring the electrical conductivity; **S3** had more chemical activity and electrical conductivity than the other compounds that were being studied. In addition, **S3** had s minimum energy gap, signifying that it had a high chemical reactivity and low electrochemical

potential. **S3** generally had less electrophilicity and chemical potential.

Funding

This research did not receive any specific grant from fundig agencies in the public, commercial, or not-for-profit sectors.

Authors' contributions

All authors contributed to data analysis, drafting, and revising of the paper and agreed to be responsible for all the aspects of this work.

Conflict of Interest

There are no conflicts of interest in this study.

ORCID

Seta Azad Aghaward
https://orcid.org/0000-0001-6524-4960
Layla Jasim Abbas
https://orcid.org/0000-0002-0415-3587
Kawkab Ali Hussein
https://orcid.org/0000-0001-9796-0929

Supporting Information

Copies of FT-IR, ^{1}H NMR (400 MHz, DMSO-d_6) and DSC, TGA, and Mass spectra of synthesized Schiff bases.

References

[1]. Tidwell T.T., Hugo (Ugo) Schiff, Schiff bases, and a century of β-lactam synthesis, *Angewandte Chemie International Edition*, 2008, **47:**1016 [Crossref], [Google Scholar], [Publisher]

[2]. Raczuk E., Dmochowska B., Samaszko-Fiertek J., Madaj J., Different Schiff Bases—Structure, Importance and Classification, *Molecules,* 2022, **27**:787 [Crossref], [Google Scholar], [Publisher]

[3]. Eranna S.C., Panchangam R.K., Kengaiah J., Adimule S.P., Foro S., Sannagangaiah D., Synthesis, structural characterization, and evaluation of new peptidomimetic Schiff bases as potential antithrombotic agents, *Monatshefte für Chemie-Chemical Monthly*, 2022, **153**:635 [Crossref], [Google Scholar], [Publisher]

[4]. Galstyan A.S., Ghochikyan T.V., Samvelyan M.A., Frangyan V.R, Sarfraz M., Synthesis, study of the biological activity of new 1, 2, 4-Triazole derivatives and characteristics of the relationship of the structure and biological activity in a series of the latter, *ChemistrySelect*, 2019, **4**:12386 [Crossref], [Google Scholar], [Publisher]

[5].S.A.Deodware,U.B.Barache,U.B.Chanshetti,D.J. Sathe, U. P. Ashok, S. H. Gaikwad, S.P.Kollur, *ResultsinChemistry*, 2021, **3**:100162 [Crossref], [Google Scholar], [Publisher]

[6]. Mironov M.E., Rybalova T.V., Pokrovskii M.A., Emaminia F., Gandalipov E.R., Pokrovskii A.G., Shults E.E., Synthesis of fully functionalized spirostanic 1,2,3-triazoles by the three component reaction of diosgenin azides with acetophenones and aryl aldehydes and their biological evaluation as antiproliferative agents, Steroids, 2022, 109133 [Crossref], Publisher]

[7]. Hozien Z.A., El-Mahdy A.F., Markeb A.A., Ali L.S., El-Sherief H.A., Synthesis of Schiff and Mannich bases of new s-triazole derivatives and their potential applications for removal of heavy metals from aqueous solution and as antimicrobial agents, *RSC advances*, 2020, **10**:20184 [Crossref], [Google Scholar], [Publisher]

[8]. Raouf H., Beyramabadi S.A., Allameh S., Morsali A., Synthesis, experimental and theoretical characterizations of a 1, 2, 4-triazole Schiff base and its nickel (II) complex, *Journal of Molecular Structure*, 2019, **1179**:779 [Crossref], [Google Scholar], [Publisher]

[9]. Jiang G.W., Chang Q., Liang D.Y., Zhang Y.T., Meng Y.J., Yi Q.Q., Preparation and antitumor effects of 4-amino-1, 2, 4-triazole Schiff base derivative, *Journal of International Medical Research*, 2020, **48**:1 [Crossref], [Google Scholar], [Publisher]

[10]. Al Sheikh Ali A., Khan D., Naqvi A., Al-Blewi F.F., Rezki N., Aouad M.R., Hagar, M., Design, synthesis, molecular modeling, anticancer studies, and density functional theory calculations of 4-(1, 2, 4-triazol-3-ylsulfanylmethyl)-1, 2, 3-triazole derivatives, *ACS omega*, 2021, **6**:301 [Crossref], [Google Scholar], [Publisher]

[11]. Lemilemu F., Bitew M., Demissie T.B., Eswaramoorthy R., Endale M., Synthesis, antibacterial and antioxidant activities of

Thiazole-based Schiff base derivatives: a combined experimental and computational study, *BMC chemistry*, 2021, **15**:1 [Crossref], [Google Scholar], [Publisher]

[12]. Said M.A., Khan D.J., Al-Blewi F.F., Al-Kaff N.S., Ali A.A., Rezki N., Aouad M.R., Hagar M., New 1, 2, 3-Triazole Scaffold Schiff Bases as Potential Anti-COVID-19: Design, Synthesis, DFT-Molecular Docking, and Cytotoxicity Aspects, *Vaccines,* 2021, **9**:1012 [Crossref], [Google Scholar], [Publisher]

[13]. Pavia D.L., G. M. Lampman, G. S. Kriz, *Introduction to spectroscopy A guide for students of organic chemistry*, Thomson Learning Academic Resource center, USA, 2013, **78**:9 [Publisher]

[14]. Stuart B.H., *Biological applications of infrared spectroscopy*, John Wiley & Sons, 1997 [Crossref], [Google Scholar], [Publisher]

[15]. Clougherty L., Sousa, J., Wyman G., C= N stretching frequency in infrared spectra of aromatic azomethines, *The Journal of Organic Chemistry,* 1957, **22**:462 [Crossref], [Google Scholar], [Publisher]

[16]. Stuart B.H., *Infrared Spectroscopy: Fundamentals and Applications*, John Wiley& Sons Ltd, USA. 2004 [Crossref], [Google Scholar], [Publisher]

[17]. Rachelle P.M., Warren S.V., Glenn G.O., In vitro cytotoxic potential of Yacon (Smallanthus sonchifolius) against HT-29, MCF-7 and HDFn cell lines, *Journal of Medicinal Plants Research,* 2017, **11**:207 [Crossref], [Google Scholar], [Publisher]

[18]. Zahedifard M., Lafta Faraj F., Paydar M., Yeng Looi C., Hajrezaei M., Hasanpourghadi M., Kamalidehghan B., Abdul Majid N., Mohd Ali H., Ameen Abdulla M., Synthesis, characterization and apoptotic activity of quinazolinone Schiff base derivatives toward MCF-7 cells via intrinsic and extrinsic apoptosis pathways, *Scientific reports*, 2015, **5**:11544 [Crossref], [Google Scholar], [Publisher]

[19]. De Los Reyes M.M., Oyong G.G., Ng V.A.S., Shen C.C., Ragasa C.Y., *Pharmacogn* J, 2017, **9**:8 [Publisher]

[20]. Mokhtar M., Alghamdi K.S., Ahmed N.S., Bakhotmah D., Saleh T.S., Design and green synthesis of novel quinolinone derivatives of potential anti-breast cancer activity against MCF-7 cell line targeting multi-receptor tyrosine kinases, *Journal of Enzyme Inhibition and Medicinal Chemistry*, 2021, **36**:1453 [Crossref], [Google Scholar], [Publisher]

[21]. Elhady S.S., Abdelhameed R.F., El-Ayouty M.M., Ibrahim A.K., Habib E.S., Elgawish M.S., Hassanean H.A., Safo M.K., Nafie M.S., Ahmed S.A., New antiproliferative triflavanone from Thymelaea hirsuta—Isolation, structure elucidation and molecular docking studies, *Molecules*, 2021. 26:739 [Crossref], [Google Scholar], [Publisher]

[22]. Morris G.M., Huey R., Lindstrom W., Sanner M.F., Belew R.K., Goodsell D.S., Olson A.J., AutoDock4 and AutoDockTools4: Automated docking with selective receptor flexibility, *Journal of computational chemistry*, 2009, **30**:2785 [Crossref], [Google Scholar], [Publisher]

[23]. BArjmand B., Hamidpour S.K., Alavi-Moghadam S., Yavari H., Shahbazbadr A., Tavirani M.R., Gilany K., Larijani B., Molecular Docking as a Therapeutic Approach for Targeting Cancer Stem Cell Metabolic Processes, *Frontiers in pharmacology*, 2022, **13**:1 [Crossref], [Google Scholar], [Publisher]

[24]. Frisch M.J., Trucks G.W., Schlegel H.B., Scuseria G.E., Robb M.A., Cheeseman J.R., Scalmani G., Barone V., Mennucci B., Petersson G.A., Nakatsuji H., Caricato M., Li X., Hratchian H.P., Izmaylov A.F., Bloino J., Zheng G., Sonnenberg J.L., Hada M., Ehara M., Toyota K., Fukuda R., Hasegawa J., Ishida M., Nakajima T., Honda Y., Kitao O., Nakai H., Vreven T.,. Montgomery Jr.J.A., Peralta J.E., Ogliaro F., Bearpark M., Heyd J.J., Brothers E., Kudin E.N., Staroverov V.N., Kobayashi R., Normand J., Raghavachari K., Rendell A., Burant J.C., Iyengar S.S., Tomasi J., Cossi M., Rega N., Millam J.M., Klene M., Knox J.E., Cross J.B., Bakken V., Adamo C., Jaramillo J., Gomperts R., Stratmann R.E., Yazyev O., Austin A.J., Cammi R., Pomelli C., Ochterski J.W., Martin R.L., Morokuma K., Zakrzewski V.G., Voth G.A., Salvador P.A., Dannenberg J.J., Dapprich S., Daniels A.D., Farkas O., Foresman J.B., Ortiz J.V., Cioslowski J., Fox D.J., Gaussian 09, Revision A.1. Gaussian, Inc., Wallingford, 2009. [Crossref], [Google Scholar], [Publisher]

[25]. Madkour L.H., Elshamy I.H., Experimental and computational studies on the inhibition performances of benzimidazole and its derivatives for the corrosion of copper in nitric acid, *International Journal of Industrial Chemistry*, 2016, **7**:195 [Crossref], [Google Scholar], [Publisher]

[26]. Shokry H., Mabrouk E.M., Computational and electrochemical investigation for corrosion inhibition of nickel in molar sulfuric acid by dihydrazide derivatives, Part II. *Arabian Journal of Chemistry*, 2017, **10**:S3402 [Crossref], [Google Scholar], [Publisher]

[27]. Aihara J.I., Correlation found between the HOMO–LUMO energy separation and the chemical reactivity at the most reactive site for isolated-pentagon isomers of fullerenes, *Physical Chemistry Chemical Physics*, 2000, **2**:3121 [Crossref], [Google Scholar], [Publisher]

[28]. Dheivamalar S., Banu K.B., The adsorption mechanism, structural and electronic properties of pyrrole adsorbed ZnO nano clusters in the field photovoltaic cells by density functional theory, *Indian journal of pure & Applied Physics*, 2019, **57**:713 [Google Scholar], [Publisher]

[29]. Bultinck P., De Winter H., Langenaeker W., Tollenare J.P., *Computational medicinal chemistry for drug discovery*, Tollenare, *Computational Medicinal Chemistry for Drug Discovery*, Taylor & Francis, England, 2003 [Crossref], [Google Scholar], [Publisher]

[30]. Domingo L.R., Ríos-Gutiérrez M., Pérez P., Applications of the conceptual density functional theory indices to organic chemistry reactivity, *Molecules,* 2016, **21**:748 [Crossref], [Google Scholar], [Publisher]

[31]. Pearson R.G., Chemical Hardness: *Applications from Molecules to Solids.* Wiley- VCH Verlag GMBH, Weinheim, Germany, 1997 [Crossref], [Google Scholar], [Publisher]

HOW TO CITE THIS ARTICLE

Seta Azad Aghaward, Layla Jasim Abbas, Kawkab Ali Hussein. Synthesis, Characterisation, and Biological and Computational Studies of Novel Schiff Bases from Heterocyclic Molecules. *J. Med. Chem. Sci*., 2023, 6(8) 1714-1726
https://doi.org/10.26655/JMCHEMSCI.2023.8.1
URL: http://www.jmchemsci.com/article_163571.html